ELSEVIER

Nuclear Physics A630 (1998) 223c–230c

NUCLEAR PHYSICS A

Quantum fluctuation effects on nuclear and atomic cluster formation

A. Ohnishi[a], Jørgen Randrup[b]* Y. Hirata[a], N. Otuka[a], Y. Nara[c], and T. Harada[d]

[a]Department of Physics, Hokkaido University, Sapporo 060, Japan

[b]Nuclear Science Division, Lawrence Berkeley Laboratory, Berkeley, CA 94720, USA

[c]Advanced Science Research Center, JAERI, Tokai, Ibaraki 319-11, Japan

[d]Department of Social Information, Sapporo Gakuin University, Ebetsu 069, Japan

The effects of quantum fluctuations on various fragmentation reactions, from the production of intermediate mass fragments in Au+Au collisions to atomic cluster formation, are studied by using the recently developed Quantal Langevin model. The larger fluctuations and the intrinsic distortion enhances fragments with low excitation energies. The fragmentation patterns in quantal and classical simulations are discussed in terms of an effective classical temperature.

1. INTRODUCTION

Understanding the properties of various phases of hadronic matter and the associated phase transitions is one of the main goals of heavy-ion physics. At intermediate energies, the relation between multifragmentation [1-3] and the liquid-gas phase transition has recently received renewed interest, after the extraction of a caloric curve of hot nuclear matter [4] suggesting that the phase transition is of first-order.

For the understanding of this phase transition, we have to invoke models which take due account of the quantum statistical nature of the nuclear system, since the nuclear liquid phase may be characterized by its quantal statistical nature, $E^* \propto T^2$. Therefore, the applicability of semi-classical transport models, such as the Quantum Molecular Dynamics (QMD), to these phenomena can be problematic. Their equations of motion are derived from a time-dependent variational principle, which neglects the effects of energy spectrum in a wave packet. Then the resulting statistical properties are essentially classical.

To take approximate account of the quantal statistical features of the evolving nuclear system, we incorporate a stochastic term given by the recently developed *Quantal Langevin* model [5,6] into wave packet dynamics. The Quantum Langevin model has been constructed based on the requirement that the system evolves to relax towards quantum-statistical equilibrium, then it is expected to improve the description of fragment formation processes, where the quantum statistics plays an important role.

In this report, we present the basic idea of the Quantal Langevin model and apply it to various fragmentation processes — nuclear fragmentation and atomic cluster formation in

*Supported by the US DOE Office of Energy Research under Contract No. DE-AC03-76SF00098.

PII S0375-9474(97)00760-4

a canonical ensemble, intermediate mass fragment (IMF) production in Au+Au collisions, and twin-single hyperfragment production in Ξ^- absorption at rest.

2. BASIC IDEA

The starting point of our discussion is the quantal statistics at equilibrium. In the case of a microcanonical ensemble, the statistical property of the system is described by the microcanonical phase volume,

$$\Omega(E) = \mathrm{Tr}\left(\delta(E-\hat{H})\right) = \int d\Gamma\, \rho_E(\boldsymbol{Z}) \ , \quad \rho_E(\boldsymbol{Z}) = \langle \boldsymbol{Z}|\delta(E-\hat{H})|\boldsymbol{Z}\rangle \ , \tag{1}$$

where $|\boldsymbol{Z}\rangle$ represents a parameterized and normalized quantum state, and $\int d\Gamma\, |\boldsymbol{Z}\rangle\langle\boldsymbol{Z}|$ resolves unity. From this phase volume, we see that the probability to find a state $|\boldsymbol{Z}\rangle$ is proportional to $\rho_E = \langle \boldsymbol{Z}|\delta(\hat{H}-E)|\boldsymbol{Z}\rangle$. Since we are considering the evolution of wave packets, the *expectation* value of the Hamiltonian operator $\mathcal{H} = \langle \boldsymbol{Z}|\hat{H}|\boldsymbol{Z}\rangle$ is not necessarily the same as the given energy E, since wave packets are not energy eigenstates. On the other hand, a naive application of the normal variational principle to the parameterized wave packets results in the probability proportional to $\delta(E-\mathcal{H})$, if the system is ergodic enough. This corresponds to the limit where the quantal energy dispersion within one wave packet is negligible, $\sigma_E^2(\boldsymbol{Z}) \equiv \langle \boldsymbol{Z}|\hat{H}^2 - \mathcal{H}^2|\boldsymbol{Z}\rangle \to 0$.

To produce the desired equilibrium distribution $\phi(\boldsymbol{Z};t) \propto \rho_E(\boldsymbol{Z}) \equiv \exp(-\mathcal{F}_E(\boldsymbol{Z}))$, it is necessary to adopt the fluctuation-dissipation dynamics described by, for example, the Fokker-Planck equation,

$$\frac{D\phi(\boldsymbol{Z};t)}{Dt} = \left[-\sum_i \frac{\partial}{\partial q_i}\left(V_i - \sum_j M_{ij}\frac{\partial}{\partial q_j}\right)\right]\phi \ , \quad V_i = -\sum_j M_{ij}\frac{\partial \mathcal{F}_E(\boldsymbol{Z})}{\partial q_j} \ , \tag{2}$$

where $\{q_i\}$ are canonical variables satisfying $d\Gamma = \prod_i dq_i$. The second relation comes from the requirement that the equilibrium distribution should be a static solution of Eq. (2). In numerical simulations, it is easier to handle the corresponding Langevin equation,

$$\frac{Dq_i}{Dt} = V_i + \sum_j g_{ij}\zeta_j \ , \quad \boldsymbol{g}\cdot\boldsymbol{g} = \boldsymbol{M} \ , \quad \prec \zeta_i(t)\,\zeta_j(t') \succ = 2\delta_{ij}\,\delta(t-t') \ . \tag{3}$$

Here we have ignored the diffusion-induced drift term [7].

Although the stochastic term appearing here is somewhat similar to the usual random force that arises from the interaction with the heat bath, the present random force arises from the energy dispersion of each wave packet and thus has a purely quantal origin. Therefore, we refer to this random force as the *Quantal Langevin* force [6].

Once the Quantal Langevin model and its equation of motion are formulated, the statistical properties of the system are determined by the "free energy" $\mathcal{F}_E(\boldsymbol{Z})$, or the energy eigenvalue distribution within each wave packet $\rho_E(\boldsymbol{Z})$. In the following sections, we introduce an approximate method to evaluate this distribution.

3. FRAGMENTATION AT FIXED TEMPERATURE

As a preparation for the dynamical scenarios, where the energy is given, we first discuss the fragmentation properties in thermal equilibrium. We then need the partition function at the given temperature $T = 1/\beta$,

$$\mathcal{Z}_\beta = \mathrm{Tr}\left(\exp(-\beta\hat{H})\right) = \int d\Gamma\, \mathcal{W}_\beta(\boldsymbol{Z}) \ , \quad \mathcal{W}_\beta(\boldsymbol{Z}) = \langle \boldsymbol{Z}|\exp(-\beta\hat{H})|\boldsymbol{Z}\rangle \ . \tag{4}$$

The statistical weight $\mathcal{W}_\beta$ is related to the energy distribution ρ_E by the Laplace transformation. We have proposed that the *harmonic approximation* to this statistical weight,

$$\mathcal{W}_\beta(\boldsymbol{Z}) \approx \exp\left[-\frac{\mathcal{H}}{D}\left(1-e^{-\beta D}\right)\right] \ , \quad D(\boldsymbol{Z}) \equiv \sigma_E^2/\mathcal{H} \ , \tag{5}$$

gives a good description [5,6,8]. It is an improved cumulant expansion with the desired asymptotic behavior; $\mathcal{W}_\beta(\boldsymbol{Z})$ converges to a finite value less than one in the low temperature limit, $\beta \to \infty$, and reduces to a normal Boltzmann factor $\exp(-\beta\mathcal{H})$ at high temperatures. As an example, we show in Fig. 1 the energy-temperature curve calculated with the harmonic approximation based on the Antisymmetrized Molecular Dynamics(AMD) [9] wave functions. Unfortunately, we could not see the energy gap, probably because the system is too small ($A = 40$). However, it is clear that the temperature initially grows as $T \propto \sqrt{E}$ which is a typical behavior of the Fermi gas or liquid phase, and it converges to a classical line $T = 2E/3A$ + constant at high temperatures.

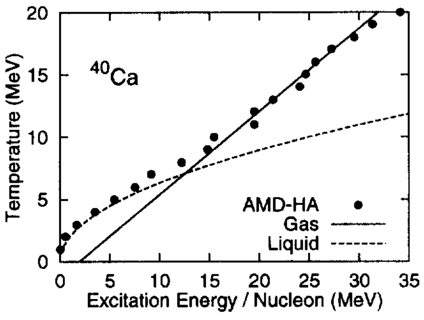

Figure 1. The mean excitation energy per nucleon E^*/A for a canonical ensemble of 40 nucleons (20 protons and 20 neutrons) confined in a sphere with a radius 2.0 fm as a function of the temperature T. Circles show the calculated results with the harmonic approximation [6] based on the AMD model. Solid and dashed lines show the temperature in gas and liquid phase. Calculated results are taken from Refs. [5,6].

Next, we apply the dynamical treatment to nuclear fragmentation [10] and atomic cluster formation [11] processes at fixed temperatures. By replacing $\mathcal{F}_E(\boldsymbol{Z})$ to $\mathcal{F}_\beta(\boldsymbol{Z}) \equiv \log(\mathcal{W}_\beta(\boldsymbol{Z}))$ in Eq. (2), the Quantal Langevin equation at a given temperature is derived. In the harmonic approximation (5), the form of the drift term is easily found,

$$V_i = -\alpha\beta\sum_j M_{ij}\frac{\partial\mathcal{H}}{\partial q_j} \ , \quad \alpha = \frac{1-\exp(-\beta D)}{\beta D} \le 1 \ , \tag{6}$$

This relation represents the *modified Einstein relation*; it deviates from the classical fluctuation-dissipation theorem which is recovered for $\alpha = 1$. Since the diffusion term becomes relatively stronger than the drift term, the Quantal Langevin force generates more fluctuations in the space of $\{q_i\}$. By using the phase space variables, $\{q_i\} = \{\boldsymbol{r}, \boldsymbol{p}\}$, the Quantal Langevin equation can now be written as,

$$\dot{\boldsymbol{p}} = \boldsymbol{f} - \alpha\beta\boldsymbol{M}^p\cdot(\boldsymbol{v}-\boldsymbol{u}) - \beta\boldsymbol{M}^p\cdot\boldsymbol{u} + \boldsymbol{g}^p\cdot\boldsymbol{\zeta}^p \ , \tag{7}$$

$$\dot{\boldsymbol{r}} = \boldsymbol{v} + \alpha\beta\boldsymbol{M}^r\cdot\boldsymbol{f} + \boldsymbol{g}^r\cdot\boldsymbol{\xi}^r \ , \tag{8}$$

$$\boldsymbol{f} \equiv -\frac{\partial\mathcal{H}}{\partial\boldsymbol{r}} \ , \quad \boldsymbol{v} \equiv \frac{\partial\mathcal{H}}{\partial\boldsymbol{p}} \ . \tag{9}$$

We have subtracted the energy dispersion related to the spurious zero-point center-of-mass motion of clusters in Eq. (7) by considering the relative velocity of each particle relative to the local collective motion with the velocity $\boldsymbol{u}$, which is close to the fragment CM motion [10,11].

In addition to the modification of the Einstein relation, we have shown that the *thermal distortion* effects on the intrinsic structure of wave packets are important in evaluating observables. The definition of the thermal average of an operator reads,

$$\prec \hat{O} \succ_\beta \;\equiv\; \frac{1}{\mathcal{Z}_\beta}\,\mathrm{Tr}\left(\hat{O}\exp(-\beta\hat{H})\right) = \frac{1}{\mathcal{Z}_\beta}\int d\Gamma\, \mathcal{W}_\beta(\boldsymbol{Z})\; \mathcal{O}_\beta(\boldsymbol{Z})\;, \tag{10}$$

$$\mathcal{O}_\beta(\boldsymbol{Z}) \;=\; \langle \boldsymbol{Z}_{\beta/2}|\hat{O}|\boldsymbol{Z}_{\beta/2}\rangle / \langle \boldsymbol{Z}_{\beta/2}|\boldsymbol{Z}_{\beta/2}\rangle\;, \quad |\boldsymbol{Z}_{\beta/2}\rangle \equiv \exp(-\beta\hat{H}/2)|\boldsymbol{Z}\rangle\;. \tag{11}$$

Thus, the thermal mean value $\prec \hat{O} \succ$ is not a weighted average of the quantum expectation value with respect to $|\boldsymbol{Z}\rangle$, but with respect to its *thermally distorted state* $|\boldsymbol{Z}_{\beta/2}\rangle$. This distortion makes the behavior of mean energy at low temperature quantal and significantly affects the nuclear fragmentation process. We have adopted the cooling equation to take this thermal distortion into account [6,10,11].

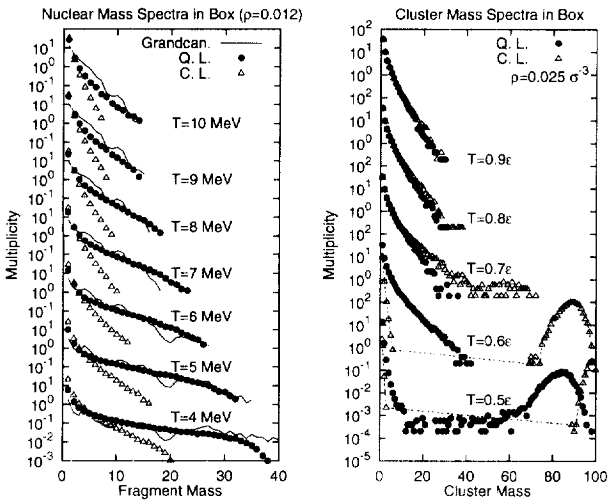

Figure 2. Nuclear (left) and cluster (right) mass distribution at given temperatures in a box. Solid circles and open triangles show the results of the simulation with the quantal and classical Langevin force, respectively. In the nuclear case, the grand canonical fragment population is also shown (solid line). Taken from Refs. [10,11].

In Fig. 2, we show the calculated nuclear fragment and atomic cluster mass distributions at given temperatures. In the nuclear case, we put 40 nucleons in a box with periodic boundary condition, and the quantal ($\alpha<1$) or classical ($\alpha=1$) Langevin force is included in the QMD model. In the atomic case, the dynamics of 100 argon atoms interacting via a Lenard-Jones potential in a box is simulated. In the classical treatment, the thermal distortion is ignored. It is clear that the quantum fluctuation effect on the atomic cluster mass distribution is opposite to that on nuclear fragmentation. Namely, the inclusion of the quantum Langevin force produces a steeper slope in the atomic cluster mass distribution at high temperatures, and the opposite in the nuclear cases.

This difference can be intuitively understood by considering the effective temperature of the Langevin equation and the quantal distortion effects by the operator $\exp(-\beta\hat{H}/2)$ [11]. Since the atoms in clusters are well separated with each other compared with the width of wave packets, the effects of the distortion on the cluster configuration are negligible. By means of the Einstein relation, we can extract the effective classical temperature of Eq. (7) as the square of the diffusion coefficient divided by the drift coefficient,

$$T_{\text{eff}} = \frac{g^2}{\alpha\beta M} = \frac{T}{\alpha} = \frac{D}{(1-e^{-D/T})} > T \; . \tag{12}$$

This estimate ignores the correction terms from the cluster center-of-mass motion and the matrix nature of $\boldsymbol{g}$ and $\boldsymbol{M}$. A classical model calculation at this effective temperature T_{eff}, has been shown to yield results that are similar to those with the quantum fluctuation at the real temperature T [11].

On the other hand, the separation between nucleons is comparable to the wave packet width in the nuclear case. Under such a condition, the effective temperature for the distorted momentum will govern the fragment distribution. For example, in the *mechanically stable* region, the Quantal Langevin equation and the effective temperature for the distorted momentum in the fragment rest frame reads

$$\dot{\boldsymbol{p}}' = e^{-D/2T}\boldsymbol{f} - \alpha\beta\boldsymbol{M}\cdot\boldsymbol{v}' + e^{-D/2T}\boldsymbol{g}\cdot\boldsymbol{\zeta} \; , \quad \boldsymbol{p}_i'(t) \;\equiv\; \boldsymbol{p}_i(\boldsymbol{Z}_{\beta/2}(t)) \simeq \; e^{-D/2T}\,\boldsymbol{p}_i(t) \; . \tag{13}$$

$$T'_{\text{eff}} = \frac{g^2 e^{-D/T}}{\alpha\beta M} = \frac{D}{e^{D/T}-1} < T \; . \tag{14}$$

It is expected, again, that a classical calculation of nuclear fragmentation at T'_{eff} gives similar results as those with quantum fluctuation at T. However, this is true only in the *mechanically stable* region, where the second equation in (13) holds. At around the critical temperature, the thermal distortion enhances the small fluctuations generated by the Quantal Langevin force and thus causes cluster rearrangements. This is the mechanism of multifragmentation suggested by the Quantal Langevin model.

4. FRAGMENTATION IN NUCLEUS-NUCLEUS COLLISIONS

4.1. Multifragmentation in Au+Au Collisions

By using the approximate statistical weight $\mathcal{W}_\beta(\boldsymbol{Z})$ for each wave packet, we can now apply the Quantal Langevin model to the nucleus-nucleus collision, where the energy is given. The harmonic approximation described above is equivalent to assuming that each wave packet has a (discrete) Poisson energy distribution. In nucleus-nucleus collisions, the total energy is much larger than the effective level spacing $D(\boldsymbol{Z})$, and we may then adopt a continuous Poisson distribution,

$$\rho_E(\boldsymbol{Z}) \;\equiv\; \langle\boldsymbol{Z}|\delta(E-\hat{H})|\boldsymbol{Z}\rangle \;\propto\; \frac{(\mathcal{H}/D)^{E/D}}{\Gamma(E/D+1)}\exp(-\mathcal{H}/D) \; . \tag{15}$$

The drift coefficient can then be readily calculated,

$$V_i \;\simeq\; -\beta_{\mathcal{H}}\sum_j M_{ij}\frac{\partial\mathcal{H}}{\partial q_j} \; , \quad \beta_{\mathcal{H}} \equiv \frac{\partial\mathcal{F}_E}{\partial\mathcal{H}} \;=\; \frac{\mathcal{H}-E}{\sigma_E^2} \; . \tag{16}$$

It is interesting to note that the drift term acts to restore the energy: when the Hamiltonian $\mathcal{H}$ is greater than the given energy E, the drift term reduces it, and vice versa. Furthermore, since the phase volume is larger for larger $\mathcal{H}$, the dynamical trajectory usually goes through the region $\mathcal{H} > E$. Therefore, fragments are cooled down in the final stage of collision, without emitting nucleons. In other words, although the wave packet wave functions with various expectation energies can contribute in the interacting region, they are projected onto their eigenenergy component in the asymptotic region.

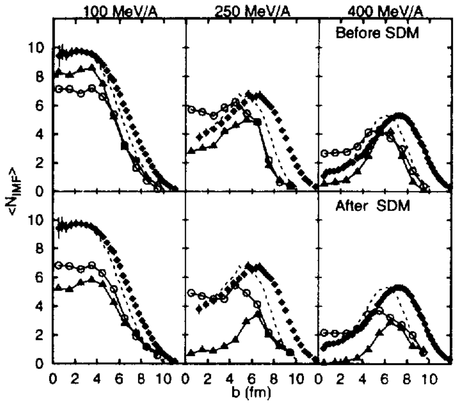

Figure 3. Circles and triangles indicate QMD results at given energies with and without the Quantal Langevin force, respectively. The upper and lower parts show the distributions before and after the statistical decay (SDM) calculation, respectively. The experimental data [1] are shown by solid diamonds. Dotted lines show the experimental data using a scaled impact parameter assuming a maximum impact parameter of 10 fm. The detector efficiency is not taken into account in the calculation. Taken from Ref. [10].

As an example, we show in Fig. 3 the calculated average multiplicity of intermediate-mass fragments in a ^{197}Au+^{197}Au collision at incident energies of 100, 250, and 400 MeV per nucleon. In the upper figure, the calculated results with QMD with and without the Quantal Langevin force are shown. Although two treatments seem to give qualitatively the same results, the excitation energies of fragments are much lower when the Quantal Langevin force is switched on. This can be seen in the lower figure, where the resulting average IMF multiplicity after the statistical decay chains are shown. In the case of QMD without the Quantal Langevin force, the excitation energies of the primary fragments are large enough to largely eliminate the IMF component from the final mass distribution. With the Quantal Langevin force, on the other hand, since a large part of the primary fragments are already cooled enough to be intact, the difference between the average multiplicities before and after the statistical decay is less than one.

4.2. Twin-Single Hypernuclear Formation in Ξ^- Absorption at Rest

The above applications show that quantum fluctuations may be important even though the systems considered have a large number of particles. Generally speaking, it is expected that the effect of the fluctuations is larger in smaller systems, as we shall now illustrate.

One of the interesting phenomena in which quantum fluctuations are desired is the hyperfragment production from Ξ^- absorption at rest, which is important for the search for double hypernucleus and H particle formation. In this reaction, the experimental data suggest the double hypernucleus formation probability of 1$\sim$ 5% [12]. In addition, two twin-single hyperfragment formation events were also observed. $^{12}\mathrm{C}+\Xi^- \to {}^{4}_{\Lambda}\mathrm{H}+{}^{9}_{\Lambda}\mathrm{Be}$ [13].

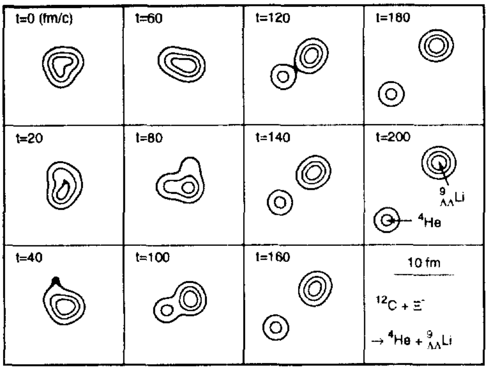

Figure 4. Density evolution in the Ξ^- absorption reaction at rest on ^{12}C calculated with the Quantal Langevin model. In this event, after partial thermalization, the relative collective motion between ^{4}He and $^{9}_{\Lambda\Lambda}$Li grows, and fragmentation occurs.

Since this fragmentation channel does not have the largest Q value, it is expected to occur during the dynamical stage, rather than at the statistical stage [14].

The energy released in the elementary process $\Xi^- p \to \Lambda\Lambda$ is around 30 MeV. This corresponds to about 3 MeV per particle if this energy is distributed in many degrees of freedom. Since this energy is smaller than the separation energy, the particle emission will be strongly suppressed in a classical treatment. In the usual AMD treatment it is calculated that a double hyper-compound nucleus is formed with a probability of more than 70%. Even after the statistical decay, the calculated formation probability of double hypernucleus formation is about 30%, which is far above the experimentally suggested value.

Therefore, we have applied the Quantal Langevin model to the Ξ^- absorption reaction on ^{12}C. Since a larger fluctuation is produced with this model, particle evaporation, including Λ evaporation, is enhanced to reduce the formation probability of double hypernuclei ($\sim$ 10% before statistical decay). In addition, the Quantal Langevin force sometimes gives almost all the excitation energy to one degree of freedom. As is shown in Fig. 4, after the relaxation of the energy initially carried by the two Λ particles to the whole nucleus, a collective motion grows and the nucleus breaks up. The final fragments are well deexcited (they become almost spherical and stable); thus we find that almost all the energy is exhausted in the relative motion between the fragments.

5. SUMMARY AND OUTLOOK

We have shown the basic idea and some applications of the Quantal Langevin model. The characteristic features of the Quantal Langevin model are the *larger fluctuations* and the *intrinsic distortion* of wave packets. The combination of these two features enhances fragments with low excitation and may modify the critical properties from those in classical treatments. The inclusion of the quantal fluctuations has led to improved results for the nuclear fragment mass distribution in the canonical ensemble, the IMF multiplicities in Au+Au collisions, and the fragmentation process from Ξ^- absorption. A shift of the critical temperature in atomic cluster formation is also suggested.

Some problems still remain in the formulation and application of the Quantal Langevin model. First, the mobility tensor $\boldsymbol{M}$ cannot be determined by statistical requirements alone, and it may be necessary to invoke other fluctuation schemes as well [15,16]. Second, it may be necessary to treat the energy dispersion related to the fragment center-of-mass motion more carefully. Finally, when antisymmetrization is imposed, the parameters of the wave packets are not canonical. Then the derivation of the dynamical equation requires the transformation matrix between the parameters and the canonical variables.

Even with these unsolved problems, the Quantal Langevin model seems promising, and it will be very exciting to attack the problem of nucleosynthesis in the early universe. While the Inhomogeneous Big Bang Nucleosynthesis (IBBN) model is expected to describe the primordial synthesis better, it has been pointed out that the fluctuations generated by the QCD phase transition might be too small to explain the abundance of light nuclei in old stars [17]. On the other hand, if the QCD phase transition makes dense baryonic matter, there is a possibility that the evolution goes through the region of spinodal instability. If so, the multifragmentation or the liquid-drop formation from this supercooled matter may make nuclei heavier than those expected in the current IBBN model. (See Fig. 5.)

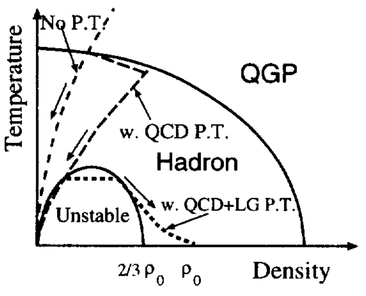

Figure 5. Phase diagram of hadronic matter and the paths of nucleosynthesis assumed in different scenarios. In the scenario, we assumed that the dense region of matter, which is created in QCD phase transition, goes through the unstable region nuclear matter.

REFERENCES

1. M.B. Tsang et al., Phys. Rev. Lett. 71 (1993) 1502.
2. K. Hagel et al., Phys. Rev. Lett. 68 (1992) 2141.
3. P. Kreutz et al., Nucl. Phys. A556 (1993) 672.
4. J. Pochadzalla et al., Phys. Rev. Lett. 75 (1995) 1040.
5. A. Ohnishi and J. Randrup, Phys. Rev. Lett. 75 (1995) 596.
6. A. Ohnishi and J. Randrup, Ann. Phys. (N.Y.) 253 (1997) 279.
7. H. Risken, *The Fokker-Planck Equation* (Springer, New York, 1989).
8. A. Ohnishi and J. Randrup, Nucl. Phys. A565 (1993) 474.
9. A. Ono et al., Phys. Rev. Lett. 68 (1992) 2898; Prog. Theor. Phys. 87 (1992) 1185.
10. A. Ohnishi and J. Randrup, Phys. Lett. B394 (1997) 260.
11. A. Ohnishi and J. Randrup, Phys. Rev. A55 (1997) 3315R.
12. S. Aoki et al., Prog. Theor. Phys. 85 (1991) 1287.
13. S. Aoki et al., Phys. Lett. B355 (1995) 45.
14. T. Yamada and K. Ikeda, Prog. Theor. Phys. Suppl. 117 (1994) 445.
15. A. Ono and H. Horiuchi, Phys. Rev. C53 (1996) 2958.
16. F. Chapelle et al., Nucl. Phys. A540 (1992) 227.
17. G.J. Mathews, T. Kajino, and M. Orito, Astrophys. J. 456 (1996) 98.